FDL-TDR-64-41
Part I

STAGNATION POINT HEAT TRANSFER IN HIGH ENTHALPY GAS FLOWS, Part I, Convective Heat Transfer in Partially Ionized Air

TECHNICAL DOCUMENTARY REPORT NO. FDL-TDR-64-41, Part I
March 1964

Flight Dynamics Laboratory
Research and Technology Division
Air Force Systems Command
Wright-Patterson Air Force Base, Ohio

Project No. 1366, Task No. 136615

(Prepared under Contract No. AF 33(657)-10110
by The Ohio State University, Columbus, Ohio;
Robert M. Nerem and George H. Stickford, authors)

FOREWORD

This report was prepared by The Ohio State University Research Foundation under USAF Contract No. AF33(657)-10110. The contract was initiated under Project No. 1366, "Aerodynamics and Flight Mechanics," Task No. 136615, "Mechanisms and Magnitudes of Aerodynamic Heating at Hypervelocities." The work was administered under the direction of the Flight Dynamics Laboratory, Research and Technology Division, Mr. L. E. Hooks, Project Engineer.

This report covers work conducted from February 1963 to February 1964.

The authors wish to express their appreciation for the encouragement and support of Dr. John D. Lee, Director, The Ohio State University Aerodynamic Laboratory.

ABSTRACT

Using an arc driven shock tube facility, measurements of convective heat transfer at the stagnation point of a blunt body have been carried out at simulated flight velocities ranging from 20,000 to 40,000 feet per second. These measurements were performed using standard calorimeter techniques with air as the test media.

The present results indicate no significant ionization effects on aerodynamic heating and indicate that the Lee's approximate equation for stagnation point heat transfer can be used for engineering calculations at flight velocities up to 40,000 feet per second.

PUBLICATION REVIEW

This report has been reviewed and is approved

FOR THE DIRECTOR

Demetrius Zonars

DEMETRIUS ZONARS
Ass't for Experimental Simulation
Flight Mechanics Division
AF Flight Dynamics Laboratory

TABLE OF CONTENTS

TABLES

ILLUSTRATIONS

SYMBOLS

a_1 = speed of sound driven tube gas

c_{p_w} = specific heat constant pressure of gas adjacent to body surface

C = specific heat for gage material

C_1 = Fay and Riddell recombination parameter

$\frac{du_1}{dx}$ = stagnation point velocity gradient

h_w = static enthalpy of gas adjacent to body surface

h_{t_o} = total enthalpy of gas flow

I = current

ℓ = gage thickness

M_s = moving shock Mach number, V_s/a_1

$Nu = \frac{\dot{q}_w \times c_{p_w}}{K_w(h_{t_o}-h_w)}$

P_1 = initial pressure driven tube

P_2 = pressure behind moving normal shock

P_s = stagnation point pressure

Pr_w = Prandtl number of gas adjacent to body surface

$\dot{q}_w$ = heat transfer rate to body

R_N = blunt body nose radius

$\mathcal{R}$ = universal gas constant

R = specific gas constant

R_o = gage resistance at reference temperature

$Re_x = \frac{u_1 x}{\nu_w}$

SYMBOLS (continued)

t	=	time
T_s	=	stagnation temperature
T_w	=	blunt body surface temperature
u_1	=	velocity at boundary layer edge
V_∞	=	flight velocity
V_s	=	moving normal shock velocity
x	=	coordinate along body surface
Z	=	compressibility factor for gas adjacent to body surface
αR_o	=	change in gage resistance with temperature
Δ	=	shock detachment distance
ΔE	=	change in voltage drop across heat transfer gage
μ_w	=	viscosity of gas adjacent to body surface
ν_w	=	kinematic viscosity of gas adjacent to body surface
ρ_2/ρ_1	=	density ratio across moving normal shock
ρ_s	=	stagnation point density
ρ_∞	=	free stream density for free flight condition
ρ	=	density gage material

I. INTRODUCTION

The heat transfer associated with the atmospheric re-entry of a space vehicle traveling at super-orbital or hyper-velocities is characterized by two key aspects. One of these is the presence of ions and electrons in appreciable amounts in the stagnation region which, in influencing transport properties, may have an effect on the aerodynamic heating rates. The second aspect is that of the increased importance of radiative heating. Both of these phenomena have received considerable attention during the past two years; however, there still exists some uncertainty with regard to the prediction of re-entry heating rates at super-orbital velocities.

Until 1962, the problem of stagnation point aerodynamic heat transfer in partially ionized air had been the center of considerable controversy because of the wide disagreement in the results of existing theoretical[1-4] and experimental[5-6] investigations. In particular, the theoretical results of Scala[4] and the experimental results of Warren[6] both indicated stagnation point heat transfer rates to be a factor of two or more greater than that predicted by other investigators for flight velocities in excess of the escape velocity. However, it has been shown recently[7] that the high heat transfer rates calculated by Scala[4] were due to the use of what would appear to be unreasonable transport properties. Excluding Scala's results, the aforementioned theories show moderate agreement, i.e., within 30 per cent of each other at flight velocities up to 50,000 feet per second.

The stagnation point convective heating rate data presented in this report were obtained to help define super-orbital velocity convective heating rates to the extent required for preliminary design of re-entry vehicles. These measurements were made in The Ohio State University arc-driven shock tube facility which is capable of generating hyper-velocity flows possessing total enthalpies of more than 60,000 BTU/lb_m.[8-11] Standard calorimeter techniques were used to measure the aerodynamic heating rates at the stagnation points of four sphere models at simulated flight velocities from 20,000 to 40,000 feet per second. Simulated altitudes ranged from 100,000 to 192,000 feet.

Manuscript released by the authors March, 1964, for publication as an FDL Technical Documentary Report.

II. THE ARC-DRIVEN SHOCK TUBE FACILITY

The facility in which the present experiments were performed is The Ohio State University arc-driven 4-inch shock tube facility shown in Fig. 1. This facility, which uses arc-heated helium as the driver gas, is capable of generating shock velocities in excess of 40,000 feet per second. The energy for this facility is supplied by a capacitor bank which has an energy rating of 200,000 Joules at its maximum voltage of 6000. The driven tube, which is 28 feet long, terminates in a dump tank producing a high-enthalpy, supersonic free jet in which a model may be placed for aerodynamic testing. All of the measurements reported here were obtained in this manner using untreated room air.

The operating range of the OSU facility is shown in Fig. 2 in terms of the standard shock tube parameters, the shock Mach number M_s, and the initial driven tube pressure p_1, and also in terms of the simulated altitude and flight velocity based on the simulation of total enthalpy and stagnation point pressure. Also shown are the velocity-altitude conditions simulated during this investigation and a typical re-entry trajectory for a super-orbital velocity lifting re-entry vehicle. Note the maximum shock Mach number attainable as a function of the initial driven tube pressure, and also the low density limit which is imposed by the available test duration.

It should be noted that the flight velocity simulated in the shock tube, based on total enthalpy, may be related, to an excellent approximation, with the standard shock tube parameters by the expression

$$V_\infty = V_s\sqrt{2(1-\rho_1/\rho_2)} \quad . \qquad (1)$$

Thus the flight velocity simulated depends only on shock velocity, being for all practical purposes independent of the initial driven tube pressure. The altitude simulated may then be determined from stagnation point density considerations through the use of references 12 through 14.

One important consideration in the application of shock tubes to the production of hypervelocity shock waves is the test duration available. The test duration, which decreases with increasing shock speed and decreasing tube pressure, may be quite small at the shock tube operating conditions necessary for the simulation of super-orbital velocity flight at altitudes above 100,000 feet. It is thus important that measurements of the test duration available be carried out for any particular facility. Extensive measurements of this type have been made in The Ohio State University facility and these are reported in reference 11. In addition, the variation in hot gas radiative emission was monitored on each run during the present program in order to obtain information on the test duration for that particular run. A random sample of test duration data obtained in this manner during the present experiments is presented in Fig. 3 for initial driven tube pressures of 1 mm Hg and 60 microns.

Fig. 1. Arc-driven shock tube facility

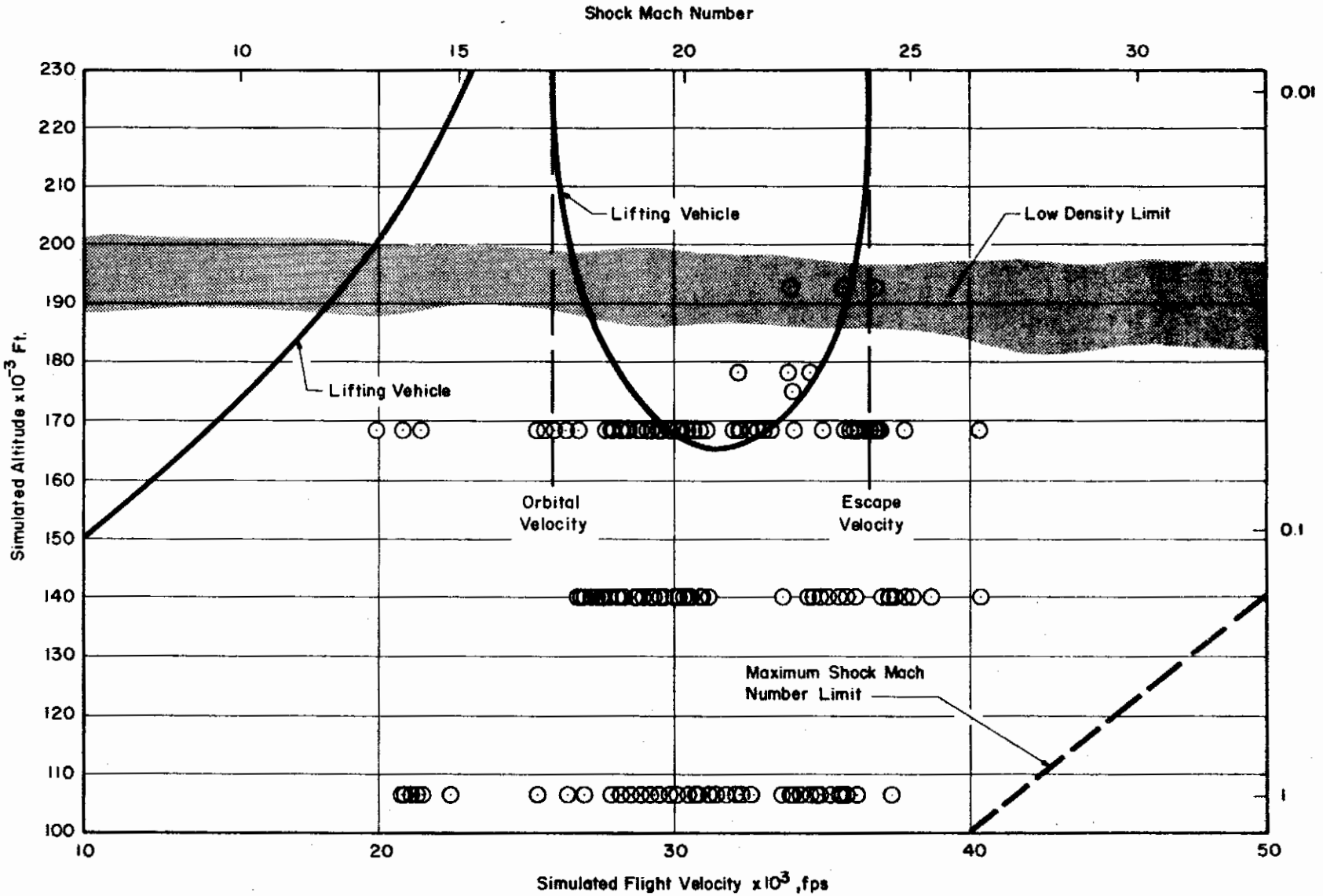

Fig. 2. Operating range for The Ohio State University arc-driven shock tube facilities, including flight conditions simulated

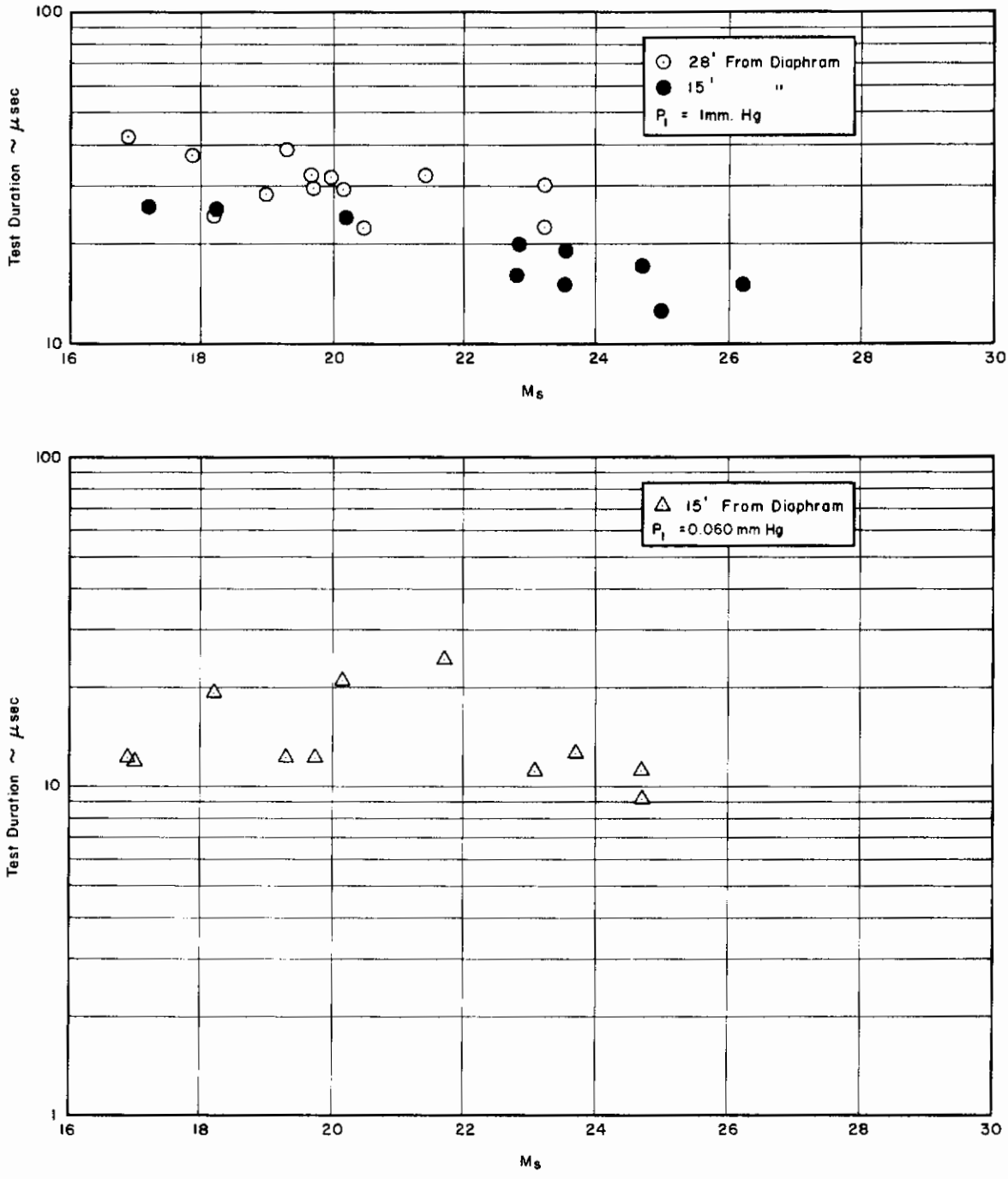

Fig. 3. Arc-driven shock tube test duration measurements

Also shown are some data from reference 11 for a position 15 feet from the diaphragm station. Since it takes on the order of 5 microseconds, depending on the configuration being tested, to establish steady flow conditions in the nose region of a model, a test duration on the order of 10 microseconds should be taken as the minimum allowed for obtaining usable data. It can be seen that in general such a test duration is available. Data obtained during the present program have been disregarded for runs for which the test duration is believed to be insufficient.

A more complete description of this facility may be found in references 8-11, while similar shock tube facilities are reported in references 6 and 15.

III. MEASUREMENTS OF AERODYNAMIC HEATING

Stagnation point aerodynamic heat transfer measurements have been carried out over a range of simulated flight velocities and altitudes, and for several size models, using calorimeter heat transfer gages. The development and application of the calorimeter gage, for use in shock tube heat transfer experiments, has been discussed in detail by P. H. Rose[16,17] of the Avco-Everett Research Laboratory where much of the early development work was carried out. In essence, the calorimeter gage may be used to measure heat transfer rates by monitoring the time-rate-of-change of the gage heat content. Since this heat content is related to the average temperature of the gage, which in turn is related to the gage resistance, then the heat transfer rate may be determined by measuring the variation in gage resistance, or for a constant current circuit, the variation in voltage drop across the gage. It is important to minimize any heat loss from the gage, and thus the choice of gage thickness is critical.

The type of model used in the present experiments is shown schematically in Fig. 4. Each such model consisted of a pyrex or glass sphere, attached to a sting, and having a calorimeter gage mounted at the stagnation point. The calorimeter gages were constructed from 0.001-inch thick uncoated platinum foil.

The properties of the platinum were obtained from reference 18. The room temperature resistance of each gage was measured before use and each was also periodically checked during use. It was found that at the extreme conditions of velocity and initial driven tube pressure, the resistance of the gage sometimes changed over a period of time because of the erosive action of diaphragm particles which impact on the gage as the driver gas passes over the model at the end of the shot.

The circuit for measuring the variation in the gage resistance is shown in Fig. 5, and is the same as suggested in reference 16. Four leads are attached to each gage--two leads for the dc power circuit which provides a constant current flow, and the other two as part of the differential circuit for measuring the variation in voltage drop across the gage. The purpose of the resistors denoted by R_1 in Fig. 5 is to reduce the effects of transient voltages induced in the differential amplifier when charged particles from the partially ionized test gas impinge on the uncoated surface of the calorimeter heat transfer gage. These resistors must be several orders of magnitude smaller than the internal resistance of the differential amplifier, and several orders of magnitude larger than the calorimeter gage resistance. When these conditions exist, the particle-induced transients act as signals from an extremely high impedance source so the R_1's short them to ground. By contrast, the voltage drop across the gage due to its instantaneous resistance is a signal from a low-impedance source so it is unaffected by the R_1's. The noise voltage is thus reduced or eliminated while the signal is displayed by the oscilloscope. It was found that reasonable results are obtainable using R_1 in the range of 100 to 10,000 ohms. The best value for R_1 will depend on the

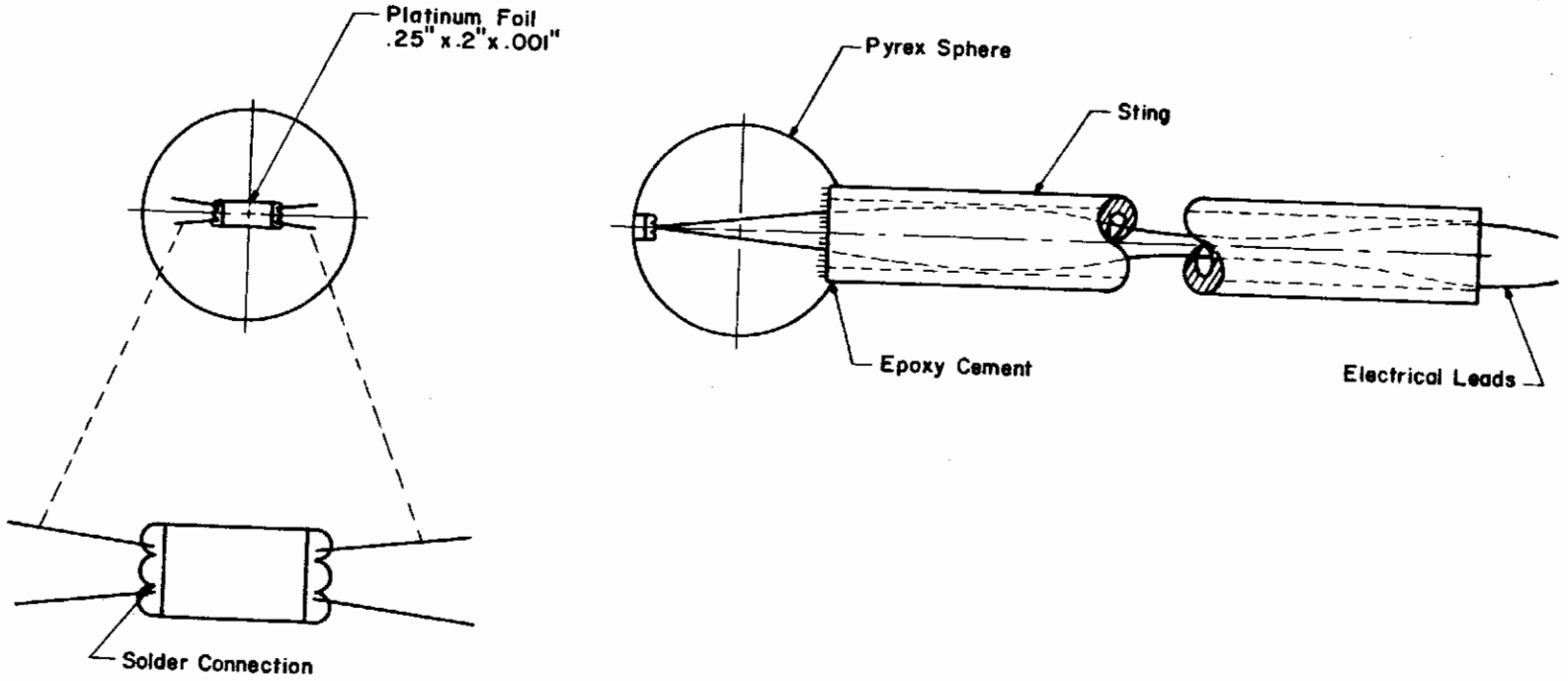

Fig. 4. Diagram of convective heat transfer model

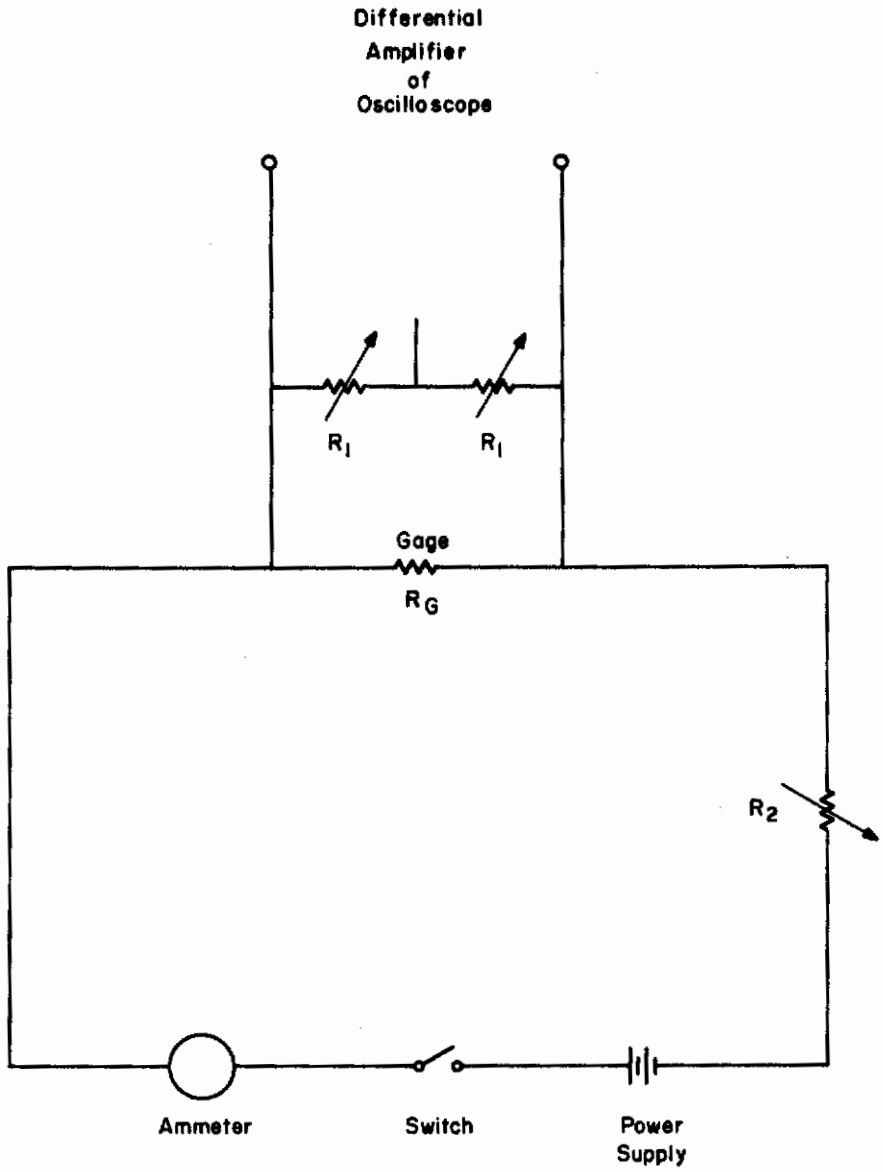

Power Supply	0-16 Volts D.C.
R_1	5000 ohms
R_2	0-10 ohms
R_G	5×10^{-3} ohms

Fig. 5. Schematic of heat transfer gage electrical circuit

particular test conditions. For the present results an R_1 of 5000 ohms was used and the two resistors were balanced to within 0.1 ohm.

The data reduction for the present measurements has been performed using the relation

$$\dot{q}_w = \frac{\rho \ell c}{\alpha R_o} \frac{1}{I} \frac{\Delta E}{\Delta t} \quad , \qquad (2)$$

where $\Delta E/\Delta t$ is the time-rate-of-change of the voltage drop across the gage, I is the gage current, and $\rho \ell c$ and $\alpha R_o = \Delta R/\Delta T$ are properties of the platinum gage material.[17,18] Corrections were applied to account for variations in gage properties with temperature, and the distribution in heat transfer over the gage, using the results of Rose.[16]

Several typical oscillograms of a calorimeter gage output are shown in Fig. 6. The vertical scale is the variation in the voltage drop across the gage, ΔE, which for a constant current in the circuit is proportional to the variation in gage resistance. The horizontal scale is time. It can be seen that following the arrival of the shock, there is a period of 3 to 5 microseconds during which the flow is non-steady and both the heat transfer rate and the induced noise level are high. It should be noted that the induced noise is the most severe at the instant the traveling normal shock passes the gage, since there is at that time no boundary layer to at least partially insulate the gage from the ionized gas surrounding it. After the flow field is established the noise becomes reduced and the gage output increases linearly with time as predicted theoretically for a constant heating rate. After 10 to 30 microseconds the contact region arrives at the gage ending the test period. This is sometimes indicated by an erratic behavior in the output of the gage, such as shown in the upper left-hand oscillogram of Fig. 6, approximately 30 microseconds after passage of the incident shock.

Note in Fig. 6, the typical gage output for the case where the circuit has not been properly balanced. In this case the two R_1 resistors are out of balance by no more than a couple of ohms out of 5000. The noise present in the gage output is due to transients induced by the ionized test gas. This induced effect becomes more important at the higher electron densities.

The majority of the results in this report are at initial driven tube pressures of 1.00, 0.20, and 0.06 mm Hg. A few additional data points were obtained at pressures less than 0.060 mm Hg. Since the available test time decreases as the initial driven tube pressure is lowered (see Fig. 3), it was extremely difficult at initial pressures less than 0.060 mm Hg to perform the heat transfer measurements under conditions where sufficient test time was available. For this reason a large number of tests were performed at these pressures in order to obtain a few usable data points.

Run No. 2534

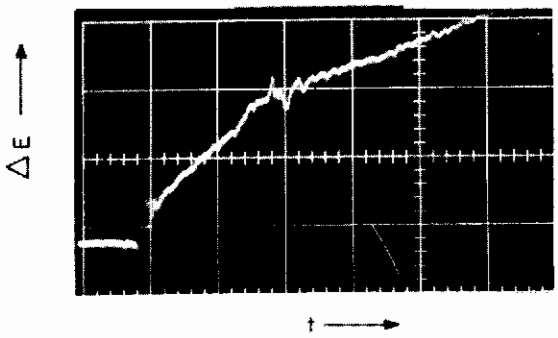

Time Scale: 20 μ sec./cm

V_s = 25,000 fps

P_1 = 1mm Hg

Run No. 2868

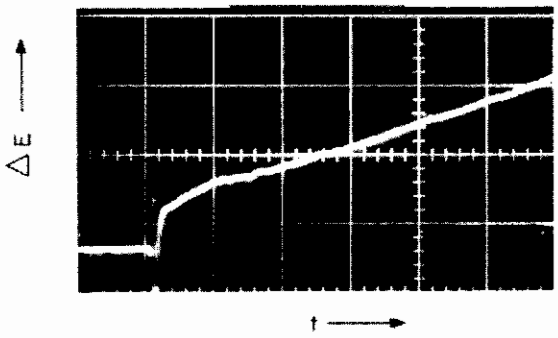

Time Scale: 20 μ sec./cm

V_s = 20,800 fps

P_1 = 0.200 mm Hg

Run No. 2553

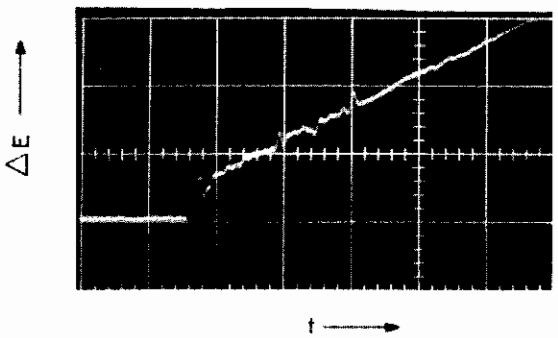

Time Scale: 10 μ sec./cm

V_s = 27,000 fps

P_1 = 0.200 mm Hg

Run No. 2530

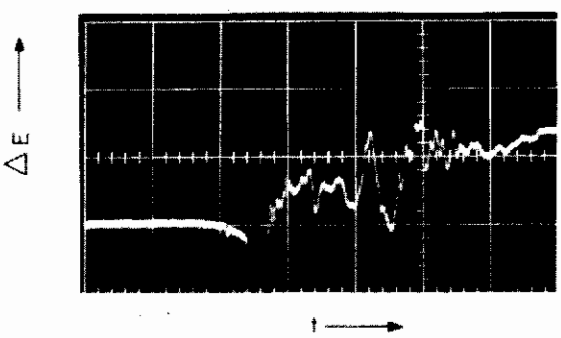

Time Scale: 20 μ sec./cm

V_s = 23,300 fps

P_1 = 1.00 mm Hg

(Noise Due to Improper Circuit Balance)

Fig. 6. Typical calorimeter gage oscillograms

Four hemispherical nose models were used in this study. The nose radii were 0.25, 0.50, 1.00, and 1.125 inches. The shock velocities ranged from 10,000 to 30,000 feet per second. The data obtained are shown in Fig. 7 - 10 and are also presented in tabular form in Tables 1-4. In Figs. 7-9, the data have been presented as $\dot{q}_w \sqrt{R_N}$ versus the shock velocity so that the dependence of the heat flux on nose radius has been removed. Because various initial driven tube pressures were used in the range below 0.060 mm Hg, these data have been plotted as $\dot{q}_w \sqrt{R_N/P_s}$ versus the shock velocity. Thus both the pressure and nose radius dependence has been taken out in the data shown in Fig. 10. These results will be analyzed in Section IV; however, it should be noted that the data scatter increases with decreasing initial driven tube pressure. This is to be expected since the measurement of the lower heat transfer rate which is associated with the lower pressure, and the measurement of the initial pressure itself, would both be expected to be less accurate.

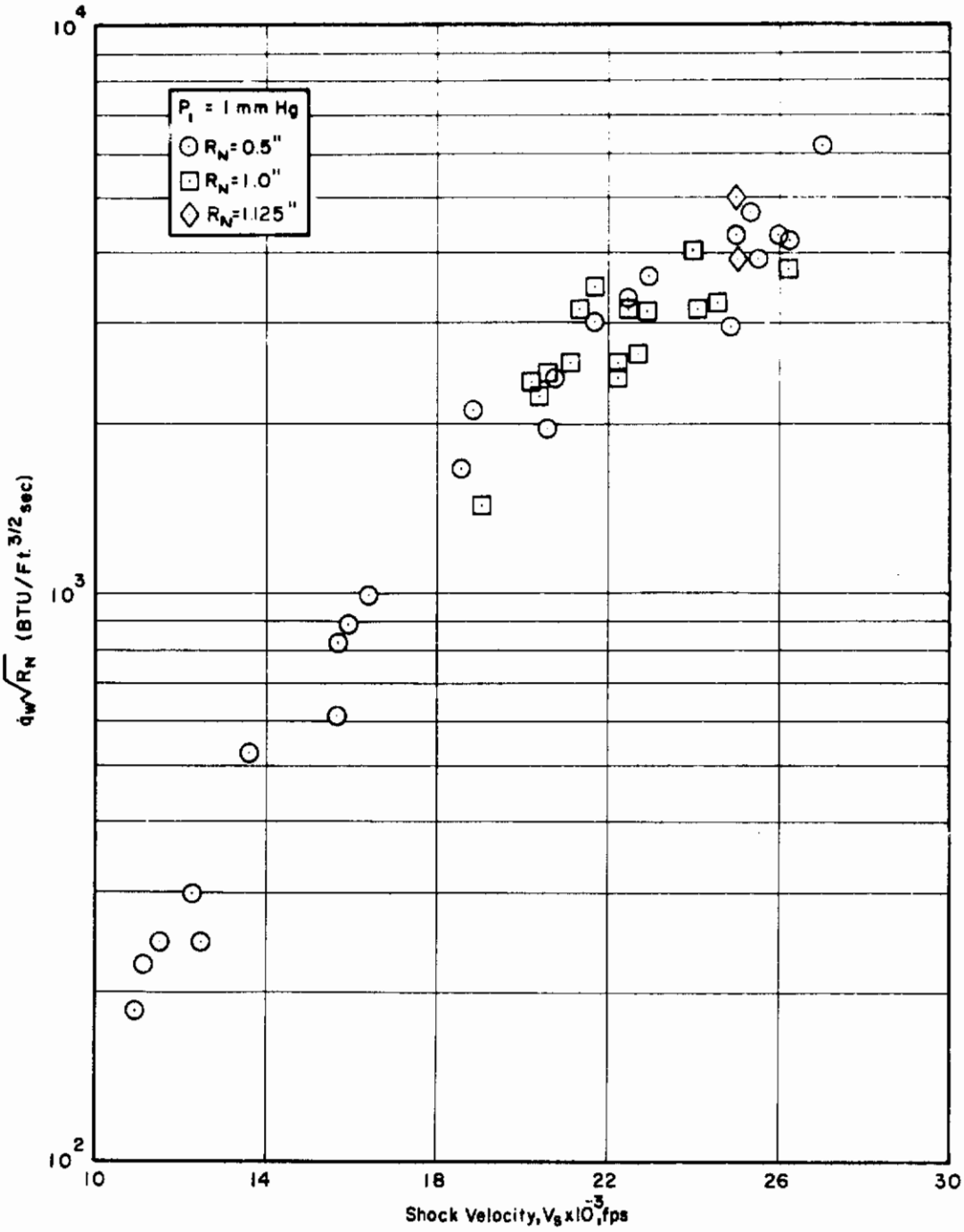

Fig. 7. Calorimeter gage heat transfer measurements, P_1 = 1 mm Hg

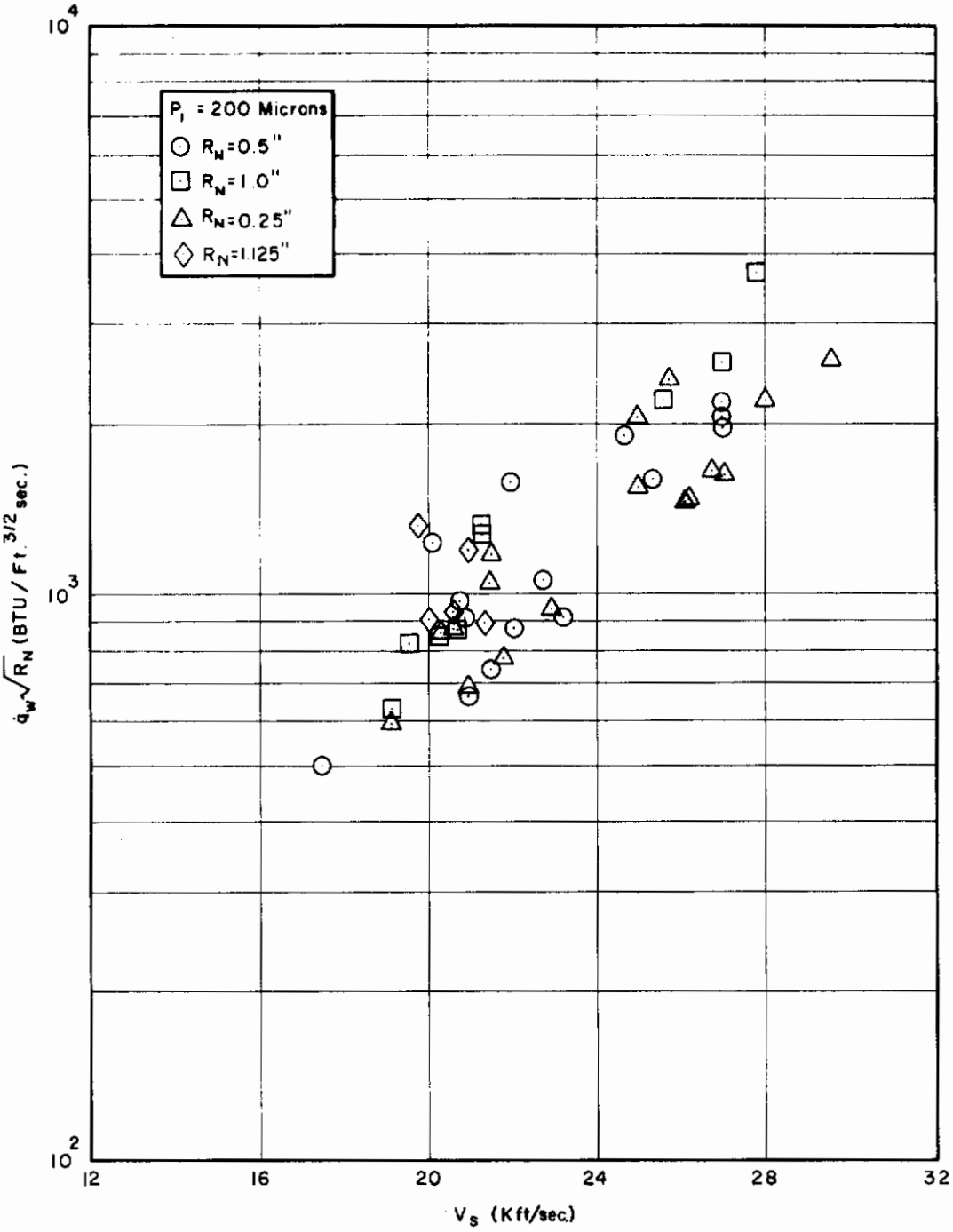

Fig. 8. Calorimeter gage heat transfer measurements, P_1 = 0.20 mm Hg

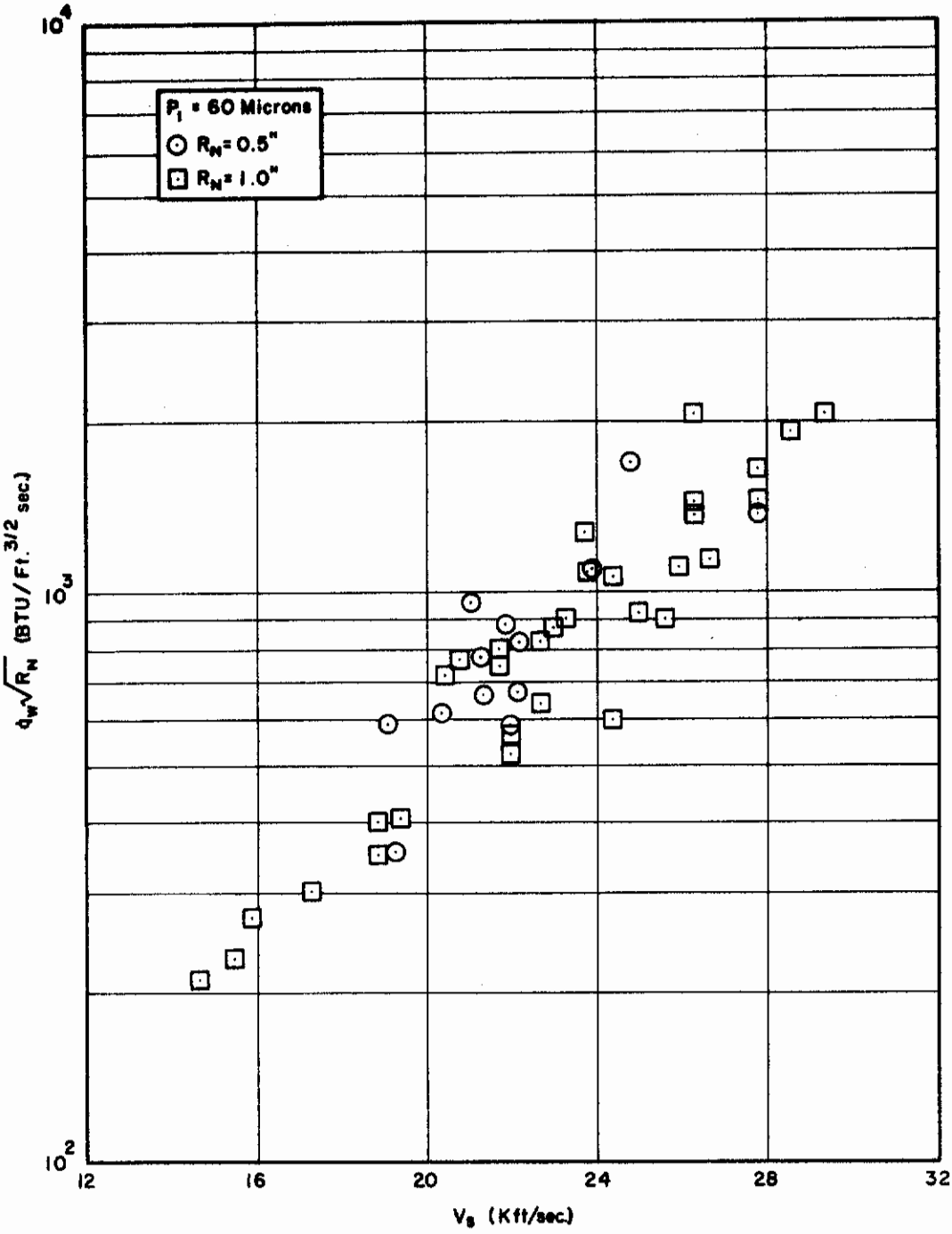

Fig. 9. Calorimeter gage heat transfer measurements, P_1 = 0.06 mm Hg

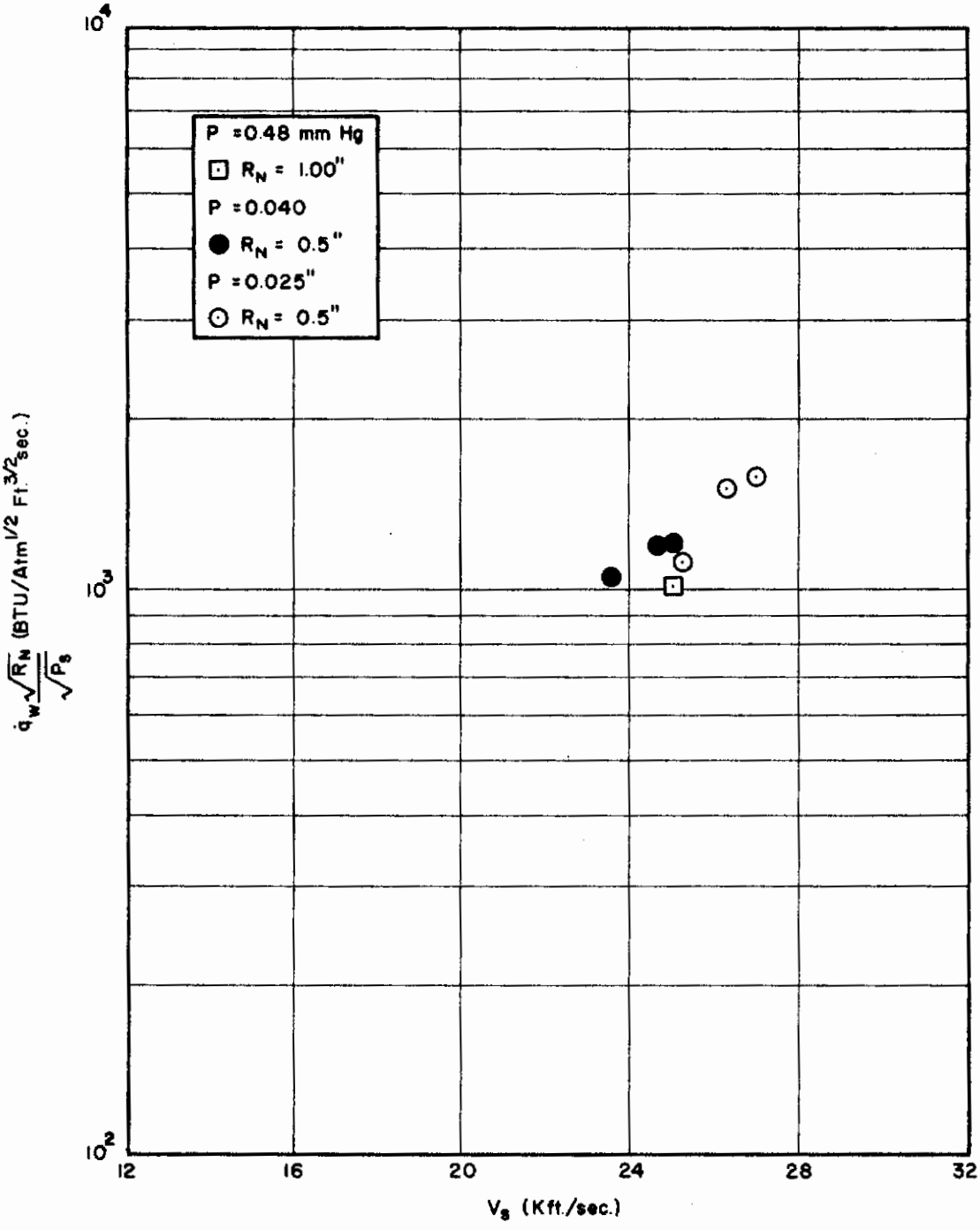

Fig. 10. Calorimeter gage heat transfer measurements, P_1 = 0.06 mm Hg

STAGNATION POINT CONVECTIVE HEAT TRANSFER DATA

TABLE 1

Nose Radius = 0.25 inch

Run No.	Shock Velocity V_s Kft/s	Initial Shock Tube Pressure P_1	Simulated Flight Velocity Kft/s	Approximate Simulated Geopotential Altitude* ft.	Simulated Free Stream Density* $x10^6$ Slugs/ft^3	$\dot{q}_w$ $x10^{-3}$ BTU/ft^2sec
2546	20.6	0.200	28.2	140,000	5.15	5.89
2547A	21.5	0.200	29.5	140,000	5.15	8.19
2547B	21.5	0.200	29.5	140,000	5.15	7.13
2549	25.0	0.200	34.3	140,000	5.15	10.5
2553	27.0	0.200	37.1	140,000	5.15	15.4
2554	25.4	0.200	34.8	140,000	5.15	13.7
2864	25.6	0.200	35.0	140,000	5.15	14.84
2865	26.0	0.200	35.6	140,000	5.15	10.20
2866	26.1	0.200	35.7	140,000	5.15	9.86
2867	29.4	0.200	40.3	140,000	5.15	18.25
2868	20.8	0.200	28.5	140,000	5.15	4.71
2869	22.7	0.200	31.1	140,000	5.15	6.45
2870	21.7	0.200	29.7	140,000	5.15	5.39

*Altitude and free stream density based on 1959 ARDC atmosphere, reference 19.

STAGNATION POINT CONVECTIVE HEAT TRANSFER DATA

TABLE 2

Nose Radius = 0.5 inch

Run No.	Shock Velocity V_s Kft/s	Initial Shock Tube Pressure P_1	Simulated Flight Velocity Kft/s	Approximate Simulated Geopotential Altitude* ft.	Simulated Free Stream Density* $\times 10^6$ Slugs/ft^3	$\dot{q}_w \times 10^{-3}$ BTU/ft^{2}sec
1985	21.7	1.00	29.7	106,000	23.6	14.8
1987	22.5	1.00	30.8	106,000	23.6	16.2
1988	23.0	1.00	31.5	106,000	23.6	17.8
1989	26.0	1.00	35.6	106,000	23.6	21.5
1990	22.3	1.00	30.4	106,000	23.6	16.2
2012A	15.7	1.00	21.1	106,000	23.6	2.98
2012B	15.7	1.00	21.1	106,000	23.6	4.11
2013	16.4	1.00	22.1	106,000	23.6	4.90
2014	15.9	1.00	21.4	106,000	23.6	4.35
2021	20.8	1.00	28.5	106,000	23.6	11.94
2025	20.6	1.00	28.2	106,000	23.6	9.67
2026	18.5	1.00	25.1	106,000	23.6	8.16
2027	18.8	1.00	25.5	106,000	23.6	10.3
2534	25.0	1.00	34.3	106,000	23.6	21.3
2540	26.3	1.00	36.1	106,000	23.6	20.1
2892	25.4	1.00	34.8	106,000	23.6	19.10
2896	24.9	1.00	34.1	106,000	23.6	14.31
2897	25.3	1.00	34.7	106,000	23.6	23.10
2899	27.4	1.00	37.5	106,000	23.6	30.65
2556	22.0	0.200	30.1	140,000	5.15	7.64
2558	17.5	0.200	23.5	140,000	5.15	2.37
2559	20.8	0.200	28.5	140,000	5.15	4.36
2560	22.7	0.200	31.1	140,000	5.15	5.17
2561	20.2	0.200	27.7	140,000	5.15	6.07
2562	20.8	0.200	28.5	140,000	5.15	4.69

TABLE 2 (continued)

Nose Radius = 0.5 inch

Run No.	Shock Velocity V_s Kft/s	Initial Shock Tube Pressure P_1	Simulated Flight Velocity Kft/s	Approximate Simulated Geopotential Altitude* ft.	Simulated Free Stream Density* $\times 10^6$ Slugs/ft^3	$q_w \times 10^{-3}$ BTU/ft^{2}sec	
2563	27.0	0.200	37.1	140,000	5.15	10.0	
2564	24.7	0.200	33.8	140,000	5.15	9.14	
2565	27.0	0.200	37.1	140,000	5.15	10.7	
2566	27.0	0.200	37.1	140,000	5.15	9.74	
2567	25.3	0.200	34.6	140,000	5.15	7.63	
2872	21.0	0.200	28.8	140,000	5.15	3.22	
2873	21.7	0.200	29.7	140,000	5.15	3.55	
2877	23.0	0.200	31.5	140,000	5.15	4.42	
2878	22.0	0.200	30.1	140,000	5.15	4.17	
2484	19,2	0.060	26.3	169,000	1.68	1.86	(N)
2485	19.1	0.060	26.0	169,000	1.68	2.86	(N)
2486	22.0	0.060	30.1	169,000	1.68	2.62	(N)
2489	22.2	0.060	30.4	169,000	1.68	3.95	(N)
2491	22.2	0.060	30.4	169.000	1.68	3.22	(N)
2903	21.7	0.060	29.7	169,000	1.68	4.35	(N)
2905	21.3	0.060	29.2	169,000	1.68	3.80	(N)
2906	20.8	0.060	28.5	169,000	1.68	4.79	(N)
2907	21.3	0.060	29.2	169,000	1.68	3.23	(N)
2908	20.2	0.060	27.5	169,000	1.68	2.99	(N)
2919	27.8	0.060	38.1	169,000	1.68	6.90	(N)
2920	23.8	0.060	32.6	169,000	1.68	5.63	(N)
2921	24.7	0.060	33.8	169,000	1.68	8.90	(N)
3035	23.5	0.040	32.3	178,000	1.22	4.10	(N)
3040	24.7	0.040	33.8	178,000	1.22	4.90	(N)
3041	25.3	0.040	34.7	178,000	1.22	4.68	(N)
3024	25.0	0.025	34.2	192,000	0.76	3.94	(N)
3026	27.0	0.025	37.0	192,000	0.76	5.40	(N)
3027	26.3	0.025	36.0	192,000	0.76	5.21	(N)

*Altitude and free stream density based on 1959 ARDC atmosphere, reference 19.
"N" indicates that chemical non-equilibrium effects may possibly be present (see discussion in Section IV).

STAGNATION POINT CONVECTIVE HEAT TRANSFER DATA

TABLE 3

Nose Radius = 1 inch

Run No.	Shock Velocity V_s Kft/s	Initial Shock Tube Pressure P_1	Simulated Flight Velocity Kft/s	Approximate Simulated Geopotential Altitude* ft.	Simulated Free Stream Density* $\times 10^6$ Slugs/ft^3	$\dot{q}_w \times 10^{-3}$ BTU/ft^{2}sec
2520	20.6	1.00	28.1	106,000	23.6	8.46
2522	21.1	1.00	28.9	106,000	23.6	8.8
2523	20.2	1.00	27.5	106,000	23.6	8.18
2524	20.4	1.00	27.8	106,000	23.6	7.82
2525	21.7	1.00	29.7	106,000	23.6	11.90
2526	21.3	1.00	29.1	106,000	23.6	11.1
2527A	22.2	1.00	30.4	106,000	23.6	8.50
2527B	19.1	1.00	25.9	106,000	23.6	5.00
2528A	22.5	1.00	30.7	106,000	23.6	11.0
2528B	22.2	1.00	30.4	106,000	23.6	8.58
2529	24.6	1.00	33.8	106,000	23.6	11.3
2531	24.1	1.00	33.0	106,000	23.6	11.1
2532	23.0	1.00	31.5	106,000	23.6	10.8
2533	22.7	1.00	31.1	106,000	23.6	9.25
2535	24.1	1.00	33.0	106,000	23.6	14.3
2538	26.2	1.00	35.9	106,000	23.6	13.0
2428	19.6	0.200	26.8	140,000	5.15	2.82
2431	21.3	0.200	29.1	140,000	5.15	4.35
2434	20.4	0.200	27.9	140,000	5.15	2.91
2435	21.3	0.200	29.1	140,000	5.15	4.42
2436	20.8	0.200	28.5	140,000	5.15	3.00
2437	25.6	0.200	35.2	140,000	5.15	7.55
2439	27.8	0.200	38.1	140,000	5.15	12.5
2440	27.0	0.200	37.1	140,000	5.15	8.67
2450	24.4	0.060	33.5	169,000	1.68	3.64 (N)

TABLE 3 (continued)

Nose Radius = 1 inch

Run No.	Shock Velocity V_s Kft/s	Initial Shock Tube Pressure P_1	Simulated Flight Velocity Kft/s	Approximate Simulated Geopotential Altitude* ft.	Simulated Free Stream Density* $\times 10^6$ Slugs/ft^3	$\dot{q}_w \times 10^{-3}$ BTU/ft^{2}sec
2454	23.3	0.060	31.9	169,000	1.68	2.69 (N)
2455	24.4	0.060	33.5	169,000	1.68	2.25 (N)
2456	22.7	0.060	31.2	169,000	1.68	2.81 (N)
2457	26.3	0.060	36.1	169,000	1.68	4.73 (N)
2459	25.6	0.060	35.2	169,000	1.68	3.13 (N)
2460	26.3	0.060	36.1	169,000	1.68	4.94 (N)
2461	26.3	0.060	36.1	169,000	1.68	7.07 (N)
2462	29.4	0.060	40.4	169,000	1.68	7.05 (N)
2463	28.6	0.060	39.2	169,000	1.68	6.52 (N)
2467	22.0	0.060	30.1	169,000	1.68	1.82 (N)
2468	23.8	0.060	32.7	169,000	1.68	4.35 (N)
2470	27.8	0.060	38.1	169,000	1.68	5.05 (N)
2471	27.8	0.060	38.1	169,000	1.68	5.65 (N)
2473	25.0	0.060	34.3	169,000	1.68	3.13 (N)
2474	26.8	0.060	36.7	169,000	1.68	3.82 (N)
2478	23.8	0.060	32.7	169,000	1.68	3.44 (N)
2479	22.7	0.060	31.2	169,000	1.68	2.78 (N)
2480	26.7	0.060	36.6	169,000	1.68	3.86 (N)
2496	20.4	0.060	27.9	169,000	1.68	2.43 (N)
2499	23.0	0.060	31.6	169,000	1.68	2.98 (N)
2503	19.4	0.060	26.7	169,000	1.68	1.34 (N)
2504	18.9	0.060	25.7	169,000	1.68	1.19 (N)
2505	21.7	0.060	29.8	169,000	1.68	2.73 (N)
2506	21.7	0.060	29.8	169,000	1.68	2.62 (N)
2509	22.0	0.060	30.1	169,000	1.68	1.92 (N)

TABLE 3 (continued)

Nose Radius = 1 inch

Run No.	Shock Velocity V_s Kft/s	Initial Shock Tube Pressure P_1	Simulated Flight Velocity Kft/s	Approximate Simulated Geopotential Altitude* ft.	Simulated Free Stream Density* $\times 10^6$ Slugs/ft^3	$\dot{q}_w \times 10^{-3}$ BTU/ft^{2}sec
2511	20.8	0.060	28.5	169,000	1.68	2.57 (N)
2513	15.5	0.060	21.0	169,000	1.68	0.782 (N)
2514	18.9	0.060	25.7	169,000	1.68	1.34 (N)
2515	15.9	0.060	21.5	169,000	1.68	0.921 (N)
2516	14.7	0.060	19.9	169,000	1.68	0.735 (N)
2518	17.3	0.060	23.4	169,000	1.68	1.05 (N)
3054	25.0	0.048	34.2	174,000	1 39	3.50 (N)

*Altitude and free stream density based on 1959 ARDC atmosphere, reference 19.

"N" indicates that chemical non-equilibrium effects may possibly be present (see discussion in Section IV).

STAGNATION POINT CONVECTIVE HEAT TRANSFER DATA

TABLE 4

Nose Radius = 1.125 inch

Run No.	Shock Velocity V_s Kft/s	Initial Shock Tube Pressure P_1 mm Hg	Simulated Flight Velocity Kft/s	Approximate Simulated Geopotential Altitude* ft.	Simulated Free Stream Density* $\times 10^6$ Slugs/ft^3	$\dot{q}_w \times 10^{-3}$ BTU/ft^{2}sec
2860	25.0	1.00	34.2	106,000	23.6	16.60
2861	25.0	1.00	34.2	106,000	23.6	12.72
2845	20.8	0.200	28.5	140,000	5.15	3.94
2846	20.0	0.200	27.4	140,000	5.15	2.91
2849	19.6	0.200	26.8	140,000	5.15	4.64
2852	21.3	0.200	29.2	140,000	5.15	2.91
2853	20.6	0.200	28.2	140,000	5.15	3.04

*Altitude and free stream density based on 1959 ARDC atmosphere, reference 19.

IV. DISCUSSION AND ANALYSIS OF RESULTS

Before making any comparison between the stagnation point heat transfer measurements reported here and the existing theoretical treatments, it is important to understand the chemical nature of the highly dissociated and even ionized flow in the stagnation region of the blunt models used in the present investigation and any resulting effect on the heat transfer rate. The questions that must be answered in considering these phenomena are: (1) is the gas at the outer edge of the boundary layer in equilibrium, chemically frozen, or reacting with a finite rate; and (2) are the recombination rates in the boundary layer rapid enough so that the boundary layer is in equilibrium at all points. Because the chemical composition affects the transport properties, which in turn affect the boundary layer profiles, a knowledge of the chemical nature is extremely important. For the case where both the inviscid flow and the boundary layer are in chemical and thermodynamic equilibrium, there will be one heat transfer rate, the equilibrium boundary layer heat transfer rate, associated with the flow. However, for the same equilibrium inviscid conditions but with a chemically frozen boundary layer and a non-catalytic wall, the heat transfer rate may be much less than the equilibrium value because of the energy involved in dissociation and ionization. Because of the non-catalytic surface effect, the wall enthalpy in this case is higher than in the equilibrium case for the same wall temperature, and the driving potential for the heat transfer, $h_{t_o}-h_w$, is reduced. It should be noted that the wall enthalpy in this case includes the energy of dissociation and ionization in addition to the normal energy modes and pressure energy.

Another example which demonstrates the importance of the effect of the chemical state on aerodynamic heat transfer is as follows:

Consider an equilibrium inviscid flow where the boundary layer is chemically frozen and the surface is highly catalytic so that the chemical state of the gas at the wall is an equilibrium one. If the inviscid stream is dissociated but un-ionized, then the heat transfer rate is unaffected by the non-equilibrium boundary layer and will be approximately equal to the equilibrium heat transfer rate. However, if the free stream is highly ionized, then the resulting heat transfer rate may be much higher than for the equilibrium boundary layer because of the transport of energy by electron and ion diffusion.

Thus it can be seen that in analyzing the results obtained in this study, it is important that consideration be given to the chemical state of stagnation region flow field. Consider first the question of whether the gas at the outer edge of the stagnation point boundary layer is in equilibrium. This can be answered by considering the relaxation process behind a normal shock. This process has been extensively studied for dissociation processes behind a normal shock moving into an undisturbed fluid[20,21]; and based on the results of such studies, Rose and Stankevics[22] have estimated the relaxation distance behind a standing shock under conditions such as encountered in the

present tests. These equilibrium distances were estimated by determining the particle time required to reach equilibrium conditions, identical to the model stagnation conditions, behind a shock moving into an undisturbed fluid, and converting this time into the distance behind the standing model bow shock. However, because the gas in front of the model bow shock is already vibrationally excited and dissociated, it would be expected that the actual relaxation distances would be shorter. Although there is presently no information in the literature that supports this, initial results obtained in this laboratory by studying reflected shocks indicate that the relaxation process for conditions such as encountered for a standing shock in a shock tube flow may be, by as much as a factor of two, more rapid than for a moving shock in an undisturbed fluid. Shown in Fig. 11 are both the calculated relaxation distances by Rose and Stankevics[22] and an estimated lower limit for the relaxation distance behind the model bow shock.

In order to determine the chemical state of the gas at the outer edge of the stagnation point boundary layer, the shock detachment distance must also be known. A recent study at this Laboratory of shock shapes in shock tube generated flows[23] indicated that in the shock Mach number range of interest here, the shock detachment distance was approximately 0.136 times the model nose radius. If the shock detachment distance is approximately equal to or greater than the chemical relaxation distance, then the gas at the outer edge of the boundary layer will be in equilibrium. From this it can be seen that for all the convective heating data taken at an initial driven tube pressure of 1 mm Hg, the gas at the outer edge of the boundary layer is in equilibrium; while at 0.200 mm Hg the gas at the outer edge of the boundary layer should be in a near equilibrium state. For all the measurements performed at 0.060 mm Hg and below, the gas is in non-equilibrium at the outer edge of the boundary layer.

Even though equilibrium conditions may prevail at the outer edge of the boundary layer, the boundary layer itself may be in non-equilibrium because of the presence of finite recombination rates. Fay and Riddell,[24] in their comprehensive treatment of the stagnation point heat transfer problem in a dissociated gas, established a parameter to measure the effect of a finite recombination rate on the boundary layer flow and on the heat transfer. Based on this parameter, Rose and Stankevics[22] analyzed the case of stagnation point heat transfer measurements in a shock tube. Their results are shown in Fig. 12 in terms of the Fay and Riddell recombination parameter, C_1, where

$$C_1 = K_1 T_s^{-3.5} \left(\frac{P_s}{R}\right)^2 \left(\frac{du_1}{dx}\right)^{-1} , \qquad (3)$$

and K_1 is a constant arising from the recombination rate of oxygen. In Fig. 12, C_1 is presented as a function of the initial driven tube pressure and for several shock velocities. For C_1 greater than unity, equilibrium boundary layer calculations should be in good agreement with experimental data because the recombination effects will be small. Frozen boundary layer calculations

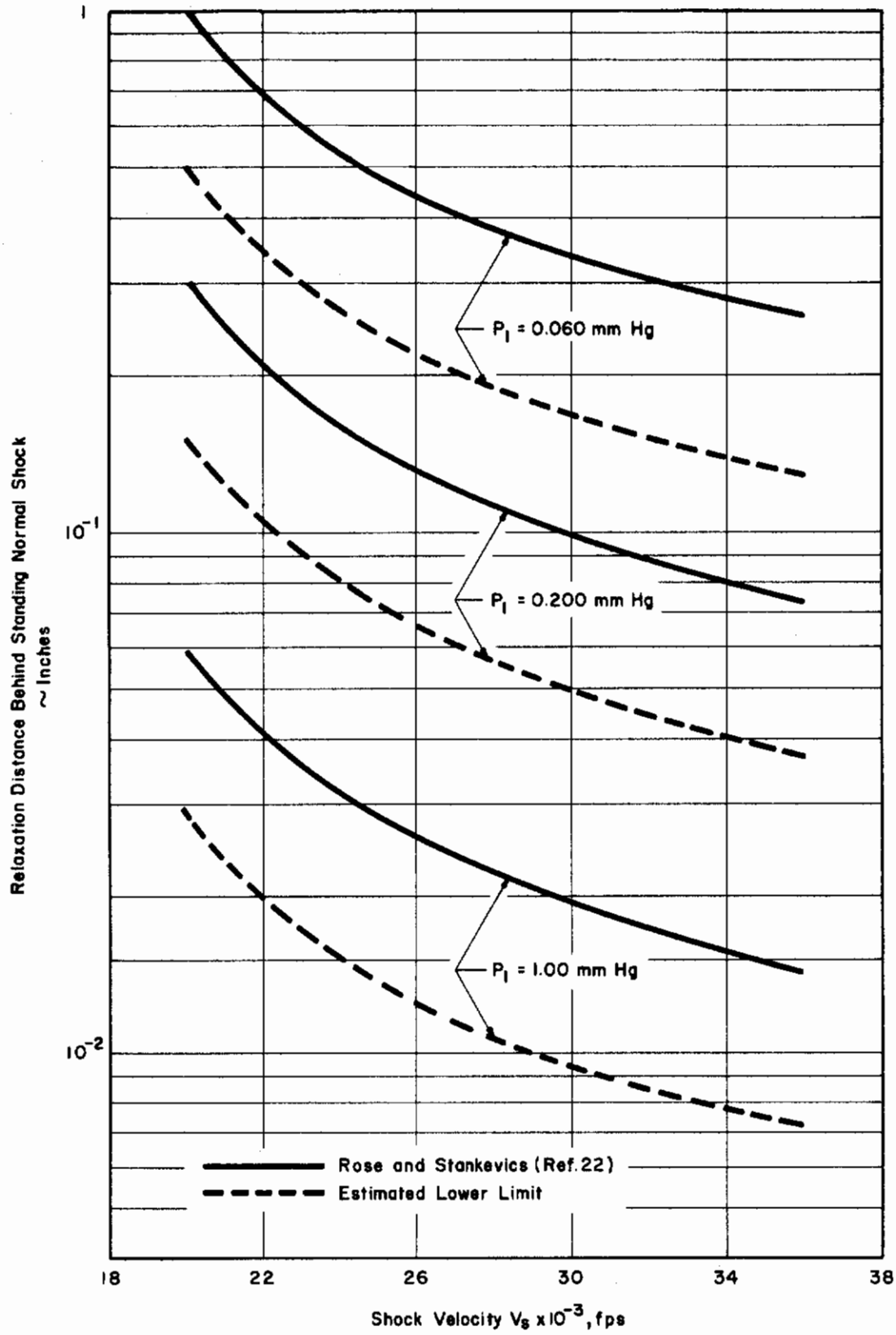

Fig. 11. Estimated relaxation distance behind standing normal shock in shock tube flow

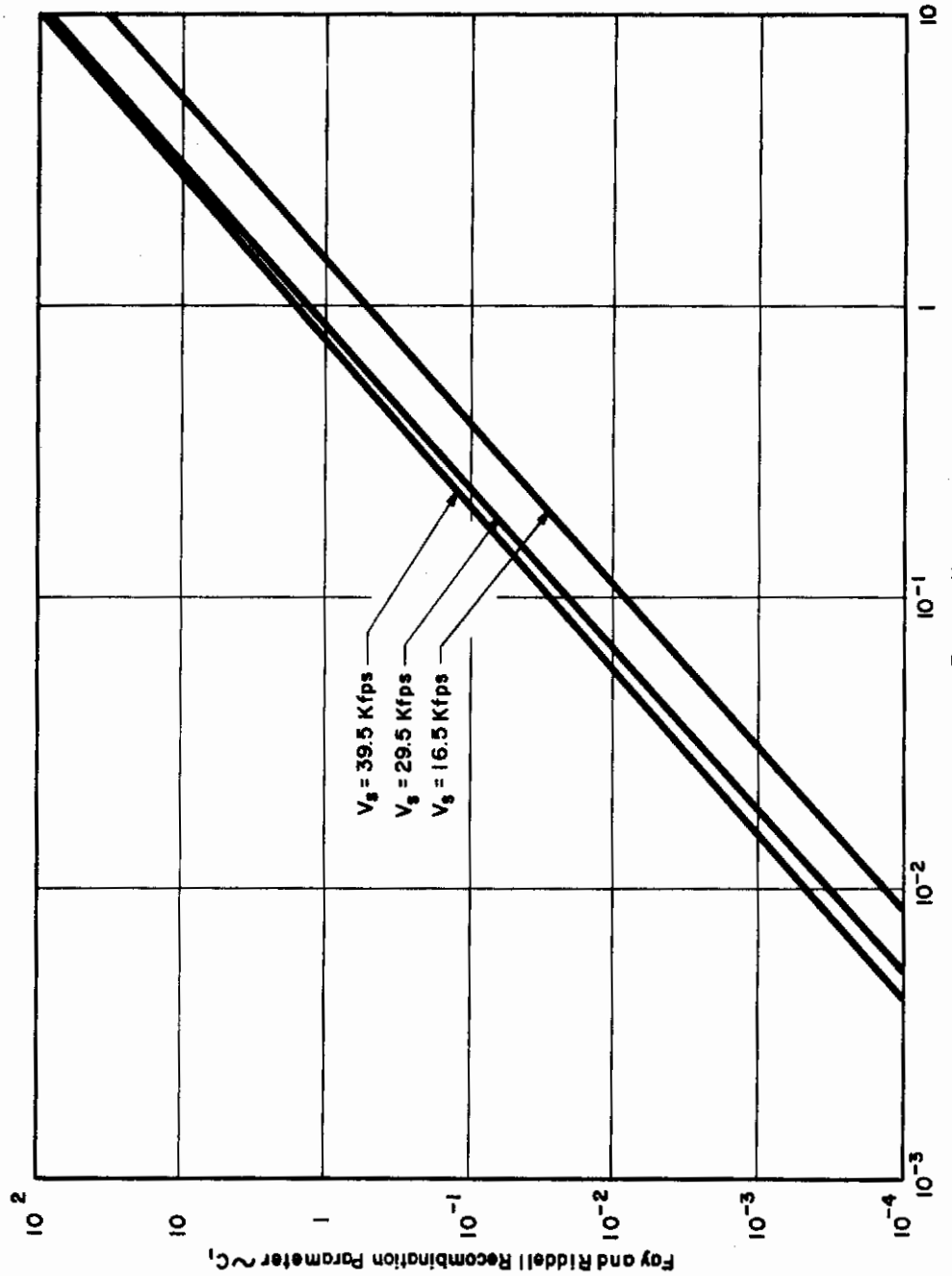

Fig. 12. Fay and Riddell recombination parameter for shock tube conditions (Reference 22)

for a catalytic surface should serve as a good approximation for C_1 less than unity. For C_1 on the order of 10^{-4} or less, surface effects will be important and must be considered. Actually the temperature dependence of the recombination rate is less than that assumed by Fay and Riddell, and Chung[25] has shown that this results in a delay in the onset of boundary layer freezing until lower densities.

It should be noted that Rose and Stankevics[22] have considered the ionization processes involved in equilibrium being attained in both the inviscid and viscid stagnation region flow; and although there is little knowledge of ionization processes at temperatures such as those attained in the present experiments, it appears that the ionization behind the shock will proceed at a faster rate than that shown in Fig. 11, and that the Fay and Riddell parameter C_1 may still be used as the governing recombination parameter in the boundary layer.

It should also be noted that most metal surfaces are catalytic, while glasses such as pyrex or quartz are non-catalytic. Although the cleanliness of a surface will affect its catalytic efficiency, the uncoated platinum foil calorimeter gages used in the present investigation are considered to be catalytic.

Based on Figs. 11 and 12, it would thus be expected that all of the convective heating results obtained at initial driven tube pressures of 1 mm Hg and 0.200 mm Hg should be at conditions where equilibrium boundary layer calculations serve as a good approximation. The data taken at 0.060 mm Hg and below would be expected to agree better with chemically frozen boundary layer calculations. These data have been identified in Tables 1-4 through the use of the symbol "N". However, it should be noted that at flight velocities below 32,000 feet per second and with a catalytic surface, for all practical purposes there is no difference between the heat transfer rate associated with a chemically frozen or an equilibrium boundary layer.[27]

A comment should be made relative to the importance of hot gas radiative heat transfer on the calorimeter gage measurements of aerodynamic heating. If a comparison is made of the radiative heat transfer rate, using the theoretical results of reference 26, and the measured convective heat transfer rate for the most extreme condition, which is a 1.0 inch radius model at a simulated velocity of 36,000 feet per second and an initial deiven tube pressure of 1 mm Hg, then it can be shown that the radiative contribution to the convective heat transfer measurements is less then 15 per cent, assuming that the calorimeter gage absorbs all the incident radiation. However, using a realistic estimate for the absorptivity of the gage, then the radiative contribution for this extreme case must be less than 10 per cent. It should be noted that initially the platinum calorimeter gages are highly reflecting; however, after a couple of runs the surface becomes grayish and has a higher absorptivity, which is estimated to be 50 per cent. For the smaller models the effect is much less since the ratio of stagnation point radiative heat transfer to convective heat transfer goes as the nose radius to the three-halves power. The effect

is also less at lower simulated flight velocities. Thus this effect has been ignored. It should be noted that a comparison of calorimeter gage measurements for models of different nose radius indicates no discernible contribution due to radiative transfer.

In correlating convective heat transfer data for laminar boundary layers, the basic parameter is the $Nu/\sqrt{Re_x}$, which may be expressed as

$$\frac{Nu}{\sqrt{Re_x}} = \frac{\dot{q}_w \sqrt{R_N}}{\sqrt{P_s}} \frac{1}{(h_{t_o} - h_w)} \left[\frac{Pr_w}{(\mu w/RTw)^{1/2}} \right] \frac{1}{\left(R_N \frac{du_1}{dx} \right)^{1/2}} \quad . \tag{4}$$

There are many theoretical solutions which result in the determination of this parameter for stagnation point boundary layers. The important solutions for ionized air or nitrogen are shown in Table 5 and are compared with the present experimental data in Fig. 13.

In calculating the $Nu/\sqrt{Re_x}$ for the experimental measurements, the inviscid gas properties were evaluated through the use of reference 13 and the velocity gradient using the modified Newtonian form

$$R_N \frac{du_1}{dx} = \sqrt{\frac{2(P_s - P_2)}{\rho 2}} \quad . \tag{5}$$

The data shown in Fig. 13 represent average values for data points obtained at approximately the same run condition. This averaging was done to reduce the data scatter and allow a more meaningful interpretation.

It can be seen in Fig. 13 that although there is general agreement with all of the theories shown, no one theory correctly predicts the level of heat transfer over the entire range of flight velocities as determined experimentally.

It was previously noted that equilibrium boundary layer calculations should serve as a good approximation for analyzing the data obtained at 1 mm Hg and 0.200 mm Hg, while chemically frozen boundary layer calculations for a catalytic surface would serve best at an initial driven tube pressure of 0.060 mm Hg. If this is the case, then it might be expected that at simulated flight velocities ranging from 30,000 to 40,000 feet per second there would be a variation in the heat transfer parameter with density. This variation is indicated by Fay and Kemp's calculations[27] of a higher value for the heat transfer parameter in a chemically frozen boundary layer than in an equilibrium boundary layer (see Fig. 13). However, there is no such variation discernible in the present experimental results. Certainly the data scatter makes any

TABLE 5

SUMMARY OF STAGNATION POINT HEAT TRANSFER CORRELATION FORMULAS

Investigator	Correlation Formula	Chemical State	Reference
Cohen	$\frac{Nu}{\sqrt{Re}} = 0.767\ (Pr_w)^{0.4} \left(\frac{\rho_1 \mu_1}{\rho_w \mu_w}\right)^{0.43} G_1(V_\infty)$	equilibrium	2
Pallone and Van Tassell	$\frac{Nu}{\sqrt{Re}} = 0.90\ (Pr_w)^{0.25} \left(\frac{\rho_1 \mu_1}{\rho_w \mu_w}\right)^{0.43} \left(\frac{V_\infty}{32500}\right)$	equilibrium	7
Hoshizaki	$\frac{Nu}{\sqrt{Re}} = 0.672\ (Pr_w) \left(\frac{T_w}{900}\right)^{0.2} \left(\frac{10^4}{V_\infty}\right)^{0.31}$	equilibrium	3

TABLE 5 (continued)

Investigator	Correlation Formula*		Chemical State	Reference
Fay and Kemp	$\frac{Nu}{\sqrt{Re}} = 0.47$	$10 < V_\infty' < 24$	equilibrium	27
	$\frac{Nu}{\sqrt{Re}} = 0.47 \left(\frac{V_\infty'}{24}\right)^{-N}$	$24 < V_\infty' < 60$		
	$\frac{Nu}{\sqrt{Re}} = 0.47$	$10 < V_\infty' < 24$		
	$\frac{Nu}{\sqrt{Re}} = 0.47 \left(\frac{V_\infty'}{24}\right)^{-0.83}$	$24 < V_\infty' < 34$	frozen	27
	$\frac{Nu}{\sqrt{Re}} = 0.35$	$34 < V_\infty' < 60$		

* $V_\infty' = \frac{V_\infty}{10^3}$ $\qquad N = 0.83 - 0.11 (\log P_s) - 0.02 (\log P_s)^2$

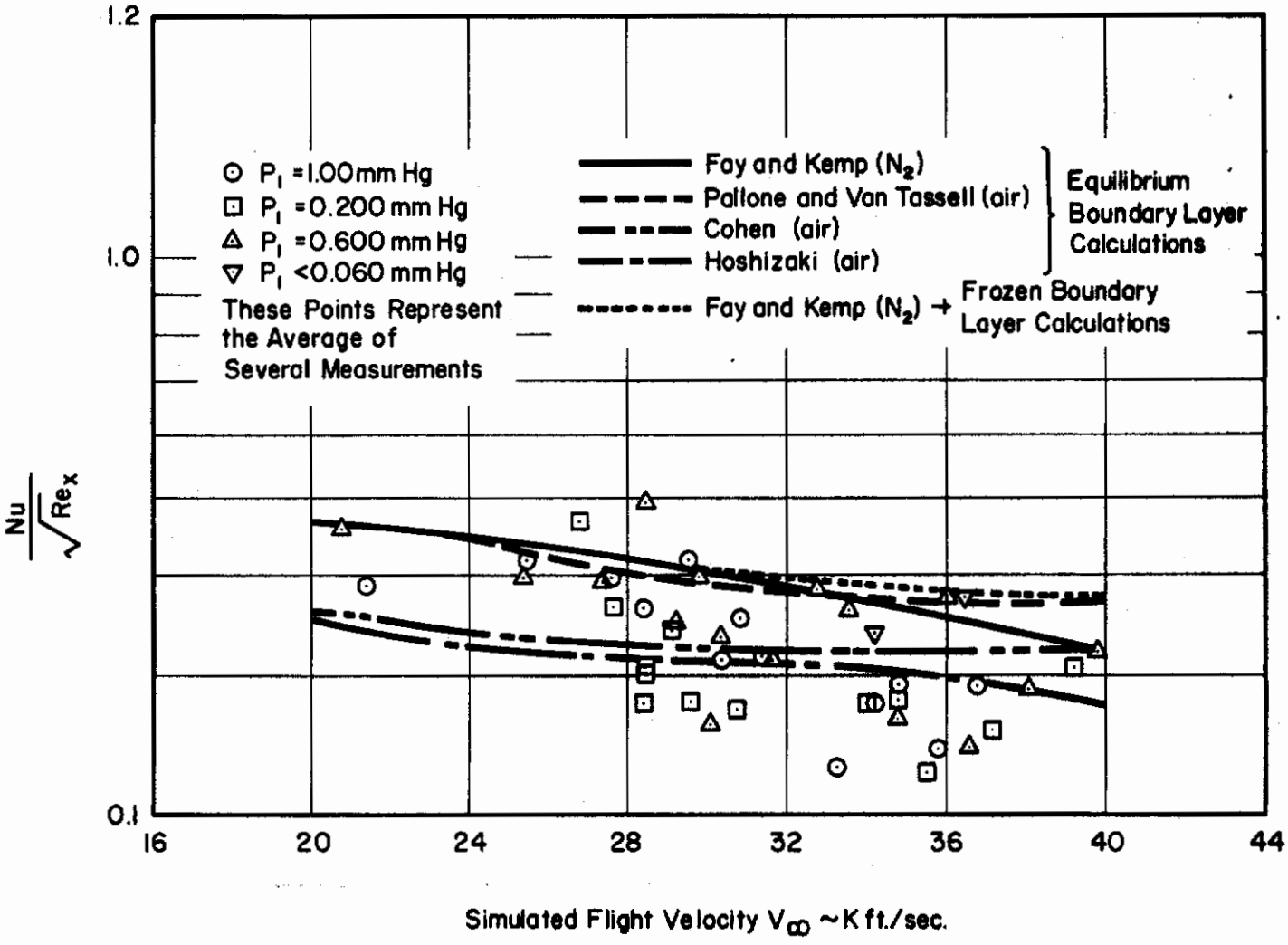

Fig. 13. Non-dimensional heat transfer parameter, $\frac{Nu}{\sqrt{Re_x}}$, versus simulated flight velocity

formal conclusion at this time rather presumptuous. It should be noted, however, that the presently accepted reaction rate for the oxygen recombination process, together with Chung's analysis, indicates a delay in the onset of boundary layer freezing as compared to Fay and Riddell's results. This would serve to explain the absence, in the present results, of any variation in the heat transfer parameter with density, since the boundary layer for all experimental conditions may be in a near-equilibrium state.

It can be seen in Fig. 13 that although no one theory is in full agreement with the experimental results, the equilibrium calculations of Fay and Kemp[27] appear to more nearly predict the correct trend. However, the predicted magnitude, when compared to the measurements, is approximately 20 per cent high over the entire range of flight velocities. It is well known that the accuracy of numerical calculation depends on the precedures used. For example, the equilibrium air calculations of Cohen,[2] Hoshizaki,[3] and Pallone and Van Tassell[7] all make use of the same transport properties yet show differences of 20 per cent or more in their results. Thus the difference between the theoretical results of Fay and Kemp and the present experimental results may be due to inherent numerical calculation inaccuracies. This same difference appears between the Fay and Kemp[27] results and the experimental data of Rose and Stankevics.[22] It thus appears that the theoretical analysis of Fay and Kemp correctly predicts the effects of ionization on stagnation point heat transfer; and although there is some question as to the magnitude of the heat transfer predicted, the chemical model used by Fay and Kemp should prove useful in other boundary layer problems.

The present experimental results are also shown in Fig. 14 in the form of $\dot{q}_w\sqrt{R_N}/\sqrt{P_s}$ as a function of $(h_{t_o}-h_w)$. The solid line has the equation

$$\frac{\dot{q}_w\sqrt{R_N}}{\sqrt{P_s}} = 47 \times 10^{-3} \quad (h_{t_o}-h_w) \quad , \qquad (6)$$

and is virtually identical to a correlation by Scala and Gilbert[28] of solutions carried out for dissociated gases of different molecular weight. It can be seen that the agreement is reasonably good (on the order of ± 20 per cent) even out at high enthalpies where ionization is appreciable. Thus for engineering purposes, the above equation should give satisfactory results in addition to being practical.

It can also be seen that there are no serious ionization effects on stagnation point aerodynamic heating at velocities up to 40,000 feet per second. This is in agreement with recent experimental results in air,[22,29] carbon dioxide,[30] and nitrogen-carbon dioxide mixtures.[31]

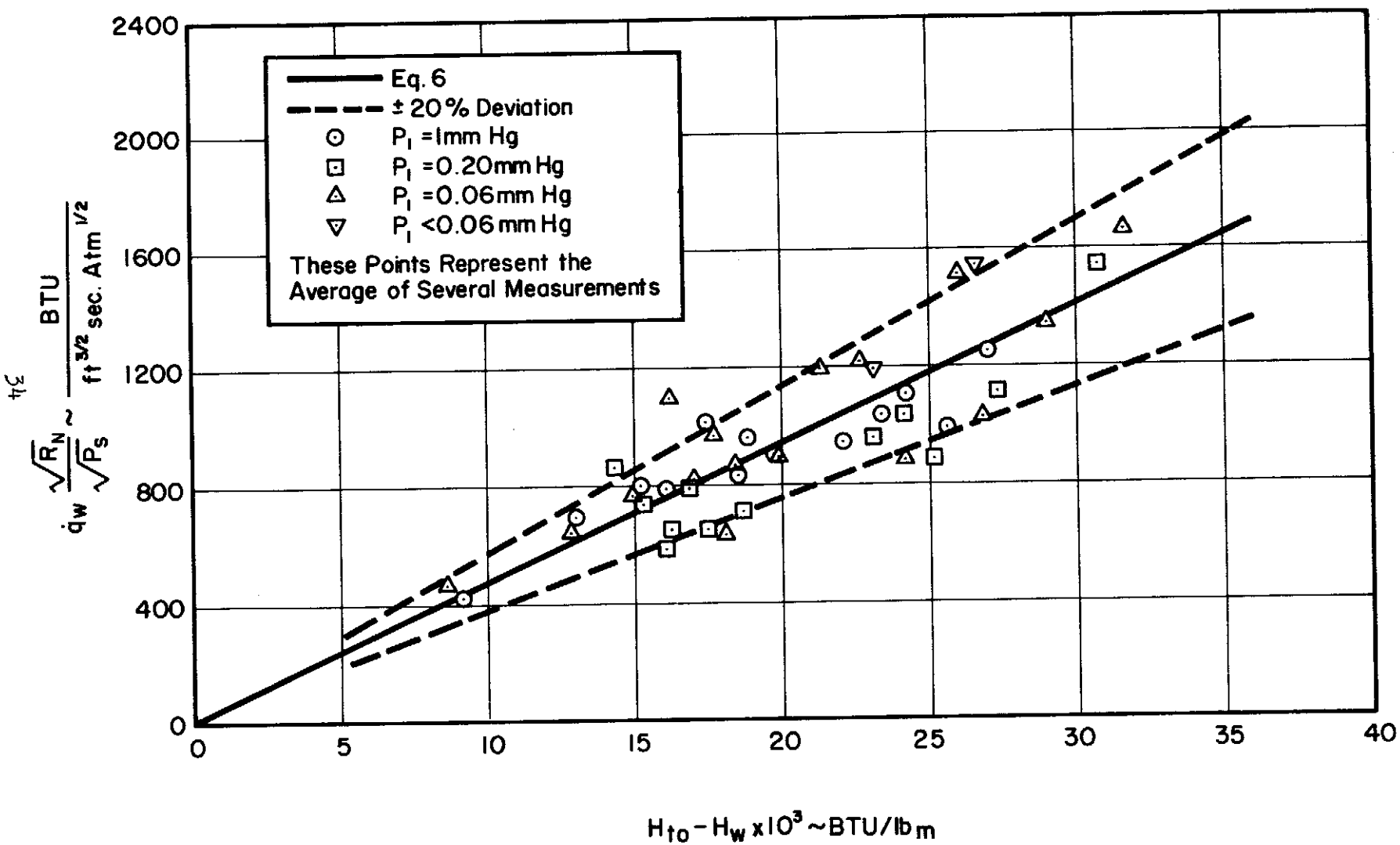

Fig. 14. High enthalpy stagnation point heat transfer correlation

Note that if h_{t_o} is replaced by $V_\infty^2/2$, and P_s by $\rho_\infty V_\infty^2$, (6) reduces to

$$\frac{\dot{q}_w\sqrt{R_N}}{\left(1-\frac{h_w}{h_{t_o}}\right)} = 20.5\ (\rho_\infty)^{1/2}\left(\frac{V_\infty}{1000}\right)^3 \quad , \tag{7}$$

which differs from the approximate form of Lee's[32] equation only in the constant, which is 21.7 in Lee's equation. Here ρ_∞ is in slugs/ft^3, V_∞ in ft/sec, R_N in ft, and $\dot{q}_w$ in BTU/ft^2/sec.

The present experimental results have been statistically analyzed by L. E. Hooks.[33] This analysis assumed first that $\dot{q}_w$, R_N, ρ_∞, and V_∞ were related by Eq. 7, and that $h_w = 6006\ (520^\circ R)$ BTU/lb$_m$. Equation 7 was solved for each of the 130 data points to yield the numerical constant. The characteristics[34] of the set of constants are as follows:

average = 20.56

non-dimensional standard deviation = 21.74%

non-dimensional skewness = 0.6416

non-dimensional kurtosis = 0.9175

(zero for a normal distribution).

Next, the exponents of R_N, ρ_∞, and V_∞ were varied to find those which gave the minimum non-dimensional standard deviation of the numerical constants, the constants being recomputed for each exponent change. The results are as follows:

$$\frac{\dot{q}_w\ R_N^{0.4116}}{\left(1-\frac{h_w}{h_{t_o}}\right)} = 12.72\ \rho_\infty^{0.4833}\left(\frac{V_\infty}{1000}\right)^{3.1536} \tag{8}$$

non-dimensional standard deviation = 21.15%

non-dimensional skewness = 0.6582

non-dimensional kurtosis = 0.7981

The exponent of V_∞ in Eq. 8 is nearly the value advocated by Detra, Kemp, and Riddell,[35] that is, 3.15. Recomputing the numerical constants from Eq. 7 with the exponent of V_∞ set to 3.15 gives

average = 12.29

non-dimensional standard deviation = 21.60%

non-dimensional skewness = 0.6327

non-dimensional kurtosis = 0.8788

On the basis of present data, no clear choice can be made among Lees' equation, Eq. 8, and Detra, Kemp, and Riddell's equation. Lees' equation, with the corrected constant of 20.5, is recommended for use in re-entry calculations at flight velocities up to 40,000 feet per second since it is the simplest of the three equations and it is a physically grounded equation rather than a curve fit.

V. CONCLUSIONS

Based on the results of this investigation, the following conclusions may be made with regard to aerodynamic heating at super-orbital velocities:

(1) There appear to be no significant ionization effects on aerodynamic heating at flight velocities up to 40,000 feet per second.

(2) The theoretical analysis of Fay and Kemp[27] appears to correctly predict the trend in the variation of the heat transfer parameter for ionized air; however, there is a 20 per cent discrepancy in the magnitude of the heat transfer as predicted by Fay and Kemp and as measured in the present experiments. Other theoretical analyses show general agreement with the present data but do not indicate the correct trend.

(3) For engineering purposes, the approximate equation of Lees[32] with a numerical constant of 20.5 is recommended. The standard deviation of the present data from this modified Lees' equation is 21.74%.

REFERENCES

1. Adams, M. C., " A Look at the Heat Transfer Problem at Super-Satellite Speeds," Avco-Everett Research Laboratory AMP 53, December, 1960. ARS Report 1556-60.

2. Cohen, N., "Boundary Layer Similar Solutions and Correlation Equations for Laminar Heat Transfer Distribution in Equilibrium Air at Velocities up to 41,100 Feet Per Second," NASA Technical Report R-118, 1961.

3. Hoskizaki, H., "Heat Transfer in Planetary Atmospheres at Super-Satellite Speeds," ARS Journal, 32, October, 1962.

4. Scala, S. M., "Heating Problems of Entry into Planetary Atmospheres from from Supercircular Orbiting Velocities," Gen. Elec. Technical Information Series R61SD176, October, 1961. (AD 282082).

5. Offenhartz, E.; Weisblatt, H.; and Flagg, R. F., "Stagnation Point Heat Transfer Measurements at Super-Satellite Speeds," Jour. Royal Aeronautical Soc., January, 1962.

6. Warren, W. R.; Rogers, D. A.; and Harris, C. J., "The Development of an Electrically Heated Shock Driven Test Facility," MSVD, General Electric TIS Report R62SD37, April, 1962.

7. Pallone, A., and Van Tassell, W., "Effects of Ionization on Stagnation-Point Heat Transfer in Air and Nitrogen," Physics of Fluids, Vol. 6, No. 7, July, 1963, pp. 983-986.

8. Lee, John D.,; and Nerem, Robert M., "Theory and Performance of a Shock Tube Having an Arc Heated Driver," The Ohio State University, Aerodynamic Laboratory Report No. 1021-18, June 15, 1962. (AD277192).

9. Caldecott, R.; Lee, J. D.; and Nerem, R. M., "The Development and Application of an Arc Driven Hypervelocity Shock Tube," Presented at the 8th Midwestern Mechanics Conference, Case Institute of Technology, Cleveland, Ohio, April 1 - 3, 1963.

10. Nerem, R. M.; Lee, J. D.; and Caldecott, R., "The Development of an Arc Discharge Driven Shock including Some Initial Results on Aerodynamic Plasmas," The Ohio State University, Aerodynamic Laboratory Report No. 1573-1, December 1, 1962, AF33(657)-10523-(AD408273).

11. Graber, B.; and Nerem, R. M., "Test Duration Measurements in an Arc Driven Hypervelocity Shock Tube," The Ohio State University, Aerodynamic Laboratory Report No. 1573-2, October 15, 1963, AF33(657)-10523-(AD423711).

12. Feldman, S., "Hypersonic Gas Dynamic Charts for Equilibrium Air," Avco Research Laboratory, Everett, Mass., 1957.

13. Ziemer, R. W., "Extended Hypervelocity Gas Dynamic Charts for Equilibrium Air," Space Technology Laboratories, Inc., Report STL/TR-60-0000-09093, 14 April 1960. (AD242694).

14. Huber, P. W., "Hypersonic Shock-Heated Flow Parameters for Velocities to 46,000 Feet Per Second and Altitudes to 323,000 Feet," NASA TR-R-163, 1963.

15. Camm, J. C.; and Rose, P. H., "Electric Shock Tube for High Velocity Simulation," Avco-Everett Research Laboratory, RR 136, July, 1962. (AD282729).

16. Rose, P. H., "Development of the Calorimeter Heat Transfer Gage for Use in Shock Tubes," Avco-Everett Research Lab. RR 17, February, 1958. (AD159547).

17. Rose, P. H., and Stack, W. I., "Stagnation Point Heat Transfer Measurements in Dissociated Air," J. Aero. Sciences, Vol. 25, No. 2 February, 1958, pp. 86-97.

18. Vines, R. F., The Platinum Metals and Their Alloys, The International Nickel Company, Inc., New York, 1941.

19. Minzner, R. A.; Champion, K. S. W.; and Pond, H. L., "The ARDC Model Atmosphere 1959, " Air Force Cambridge Research Center, AFCRC TR-59-267, August 1959. (AD229482).

20. Allen, R. A.; Rose, P. H.; and Cemm, J. C., "Non-Equilibrium and Equilibrium Radiation at Super-Satellite Re-entry Velocities," IAS Preprint No. 63-77, Presented at IAS 31st Annual Meeting, New York, January 21 - 23, 1963.

21. Teare, J. D.; Georgiev, S.; and Allen, R. A., "Radiation from the Non-Equilibrium Shock Front," Progress in Astronautics and Rocketry: Hypersonic Flow Research, edited by F. R. Riddell, Academic Press, New York, 1962.

22. Rose, P. H., and Stankevics, J. O., "Stagnation Point Heat Transfer Measurements in Partially Ionized Air," Presented at the IAS 31st Annual Meeting, New York, January 21 - 23, 1963, IAS Paper No. 63-61; also published in AIAA Journal, Vol. I, No. 12, December, 1963, pp. 2752-2763.

23. Graber, B. C., "An Experimental Study of Real Gas Effects on Shock Detachment Distances and Shock Shapes for a Group of Spherically Blunted Bodies," M. Sc. Thesis, The Ohio State University, November, 1963. (To be published as an FDL TDR, Research and Technology Division, AFSC).

24. Fay, J. A., and Riddell, F. R., "Theory of Stagnation Point Heat Transfer in Dissociated Air," J. Aero/Space Sci., Vol 25, No. 2 February, 1958.

25. Chung, P. M., "Hypersonic Viscous Shock Layer of Non-Equilibrium Dissociating Gas," NASA TR-109, 1961.

26. Nardone, M. C.; Breen, R. G.; Zeldin, S. S.; and Riethof, T. R., "Radiance of Species in High Temperature Air," GE R63SD3, General Electric Space Sciences Lab., June, 1963. (AD408564).

27. Fay, J. A., and Kemp, N. H., "Theory of Stagnation Point Heat Transfer in a Partially Ionized Diatomic Gas," Avco-Everett Research Laboratory, Research Report 144, December, 1962. (AD405723).

28. Scala, S. M., and Gilbert, L. M., "Theory of Hypersonic Laminar Stagnation Region Heat Transfer in Dissociating Gases," Present at the 8th Midwestern Mechanics Conference, Case Institute of Technology, Cleveland, Ohio, April 1 - 3, 1963.

29. Hoshizaki, H., "Convective Heating Measurements at Super-Orbital Speeds," Lockheed Missiles and Space Division, Report No. 6-90-62-50, June, 1962.

30. Nerem, R. M.; Morgan, C. J.; and Braber, B C., "Hypervelocity Stagnation Point Heat Transfer in a Carbon Dioxide Atmosphere," AIAA Journal, September, 1963, p. 2173.

31. Gruszczynski, J. S., and Warren, W. R., "Experimental Heat Transfer Studies of Hypervelocity Flight in Planetary Atmospheres," AIAA Preprint No. 63-450, Presented at AIAA Conference on Physics of Re-entry, August, 1963.

32. Lees, L., "Recovery Dynamics-Heat Transfer at Hypersonic Speed in a Planetary Atmosphere," Space Technology, ed. by H. Siefert, John Wiley and Sons, Inc., New York, 1959.

33. Hooks, L. E., Research and Technology Division, Air Force Systems Command, Wright Patterson, AFB, Dayton, Ohio. Private Communication.

34. Spiegel, M. R., Theory and Problems of Statistics, Schaum Publishing Co., New York, 1961, Chap. 5, pp. 89-92.

35. Detra, R. W.; Kemp, N. H.; and Riddell, F. R.;"Addendum to Heat Transfer to Satellite Vehicles Re-entering the Atmosphere," Jet Propulsion, December, 1957, Vol. 27, No. 4, pp. 1256-1257